C. R. Chimie 13 (2010) 515–526

Contents lists available at ScienceDirect

Comptes Rendus Chimie

www.sciencedirect.com

Full paper/Mémoire

VOCs and carbonaceous particles removal assisted by NO_x on alkali$_{0.15}$/ZrO_2 and Cs_x–$M_{0.1}$/ZrO_2 catalysts (M = Cu or Co)

Aissa Aissat [a,b], Stéphane Siffert [a,b,*], Dominique Courcot [a,b], Renaud Cousin [a,b], Antoine Aboukaïs [a,b]

[a] University Lille Nord-de-France, 59000 Lille, France
[b] ULCO, UCEIV, 59140 Dunkerque, France

ARTICLE INFO

Article history:
Received 8 June 2009
Accepted after revision 31 March 2010
Available online 14 May 2010

Keywords:
Alkali metals
VOCs oxidation
NOx conversion
Carbonaceous particles
Simultaneous removal

ABSTRACT

The effect of alkali metals on the physicochemical characteristics of zirconium oxide and the properties of alkali metals in the oxidation of toluene and/or carbonaceous particles and/or conversion of nitrogen oxides have been studied. We observed that they had an effect on the structural and textural properties of ZrO_2. These solids were tested first in the oxidation of toluene and carbonaceous particles separately and secondly with both pollutants. Whatever the experiments, the sample $Cs_{0.15}/ZrO_2$ was found to be the catalyst the most active. The simultaneous removal of toluene and soot shows that the presence of toluene leads to a decrease in the temperature of the maximum soot oxidation rate, particularly with catalysts impregnated of Cs and Cu. The effect of the Cs/Co ratio on NO_x conversion and toluene oxidation was also studied. It was found that the oxidizing properties of NO_x can increase the conversion of toluene. This phenomenon occurs especially in the presence of catalysts with a low amount of alkali metal. For the oxidation of carbonaceous particles on the samples Cs/ZrO_2 impregnated with transition metals, the best performance is obtained for copper, although a decrease of the ratio Cs/Cu leads to a slower oxidation and a shift to higher temperatures.

RÉSUMÉ

Mots clés :
Métaux alcalins
Oxydation des COV
Conversion des NOx
Particules carbonées
Élimination simultanée

L'effet d'éléments alcalins sur les caractéristiques physicochimiques de l'oxyde de zirconium (ZrO_2) et sur ses propriétés catalytiques en oxydation du toluène et/ou des particules carbonées et/ou la conversion des oxydes d'azote a été étudié. Nous avons pu observer qu'ils avaient un effet sur les propriétés structurales et texturales de ZrO_2. Ces catalyseurs ont été testés dans l'oxydation du toluène et de particules carbonées; d'une part, de manière distincte et, d'autre part, en considérant conjointement deux réactifs. Ces expériences révèlent que l'échantillon $Cs_{0.15}/ZrO_2$ est le catalyseur le plus performant. L'élimination simultanée du toluène et de particules carbonées montre que la présence du toluène mène à diminuer la température de la vitesse d'oxydation maximale de la suie, particulièrement avec des catalyseurs imprégnés avec Cs et Cu. L'effet du rapport Cs/Co dans la conversion des NO_x et l'oxydation du toluène a été étudié. Il a été trouvé que les propriétés oxydantes des NO_x permettent d'augmenter la conversion du toluène. Ce phénomène est rencontré en présence des catalyseurs avec un rapport Cs/Co petit. Pour l'oxydation des particules carbonées sur les échantillons Cs/ZrO_2 imprégnés avec les métaux de transition, nous avons observé que l'échantillon au cuivre avait la meilleure

---

* Corresponding author.
E-mail address: siffert@univ-littoral.fr (S. Siffert).

1631-0748/$ – see front matter © 2010 Académie des sciences. Published by Elsevier Masson SAS. All rights reserved.
doi:10.1016/j.crci.2010.03.027

performance, bien que la diminution du rapport Cs/Cu provoque une oxydation moins rapide et un déplacement vers des températures plus élevées.

1. Introduction

The simultaneous emission of volatile organic compounds (VOCs), nitrogen oxides (NO_x) and carbonaceous particles concerns many industries (steel, incineration, combustion of biofuels...). A catalytic treatment may be an advantageous route for the purification of such effluents [1–3].

The catalytic oxidation of VOCs to carbon dioxide and water has been identified as one of the most efficient ways to their destruction at low concentrations and to meet increasingly environmental regulations. The practical applications of the catalytic oxidation process require heating large amounts of gas containing low concentrations of VOCs to find the oxidation temperature. Therefore, highly active catalysts at low temperatures are required [4]. Moreover, the oxidation of hydrocarbons in the presence of NO_x can be interesting both for automotive pollution control and in various industrial plants [2,3]. However, the studies are usually oriented to the complete NO_x reduction in the presence of low amounts of light hydrocarbons [5–9] but not the inverse: complete oxidation of VOCs in the presence of NO_x.

The use of zirconia as oxidation catalysts has been claimed for its thermal stability and specific area [4] and also for its selectivity for NO_x reduction to N_2 [10].

The introduction of alkali metals in catalysts developed for the oxidation of hydrocarbons in the presence of NO_x is expected to provide interesting effects. In some cases, alkali metals are known to be activity promoters for the oxidation of hydrocarbons as well as for NO_x reduction [10]. Previous works of our laboratory [1,11] presented this effect of alkali metals in the oxidation of soot.

The introduction of both alkali metal and transition metal (cobalt or copper) on ZrO_2 are investigated and provided synergistic effects in the soot oxidation [11]. Moreover, cobalt and copper oxides are known to be active phases for VOCs oxidation [12–14] and also for NO_x reduction [2,15]. Co and Cu were then also impregnated on the samples for improving the catalytic behaviours.

Therefore, the aim of this work is the study of the effect of alkali elements (Li, Na, K, Rb, Cs) on the physicochemical characteristics of zirconium oxide (ZrO_2) and its catalytic properties in oxidation of toluene and/or carbonaceous particles and/or conversion of nitrogen oxides. The effects of Cs/Co and Cs/Cu ratios in the different catalytic tests were also studied.

2. Experimental

2.1. Catalysts synthesis

The zirconium oxide support was prepared by a precipitation method, adding dropwise an aqueous solution of zirconyl (IV) chloride to an ammonia solution under continuous stirring. The precipitate was filtered and washed to remove remaining chloride ions [16]. This solid was dried at 115 °C for 24 h and subsequently calcined under air flow (2 L h^{-1}) at 300 °C for 4 h [1,4,11].

The alkali/ZrO_2 systems were obtained by impregnation of aqueous alkali carbonates on a ZrO_2 support, with an initial specific area of 201 $m^2\ g^{-1}$.

Alkali–$Co_{0.1}$/ZrO_2 catalysts were prepared by co-impregnation of cobalt ($CoCO_3{\cdot}nH_2O$) and an alkali carbonate onto ZrO_2 solid. Alkali–$Cu_{0.1}$/ZrO_2 catalysts were prepared with the same method (using $CuCO_3{\cdot}nCu(OH)_2$).

After drying, the samples were calcined under air flow (2 L h^{-1}) at 600 °C for 4 h. The as-obtained solids will be denoted by alkali$_x$–$M_{0.1}$/ZrO_2 where M is the symbol of the impregnated transition metal, x and 0.1 correspond respectively to alkali/Zr and M/ZrO_2 atomic ratios.

2.2. Catalysts characterization

The chemical composition of the samples was determined by ICP–MS with a Varian 820 MS apparatus.

TG–DTA experiments were studied with a Netzsch STA 409 apparatus. About 30 mg of dried catalyst were loaded in an alumina crucible and heated from room temperature to 1000 °C (heating rate: 5 °C min^{-1}) in air flow (75 mL min^{-1}).

BET surface areas were measured by nitrogen adsorption at 77 K on a Qsurf M1 apparatus (Thermo Electron Corporation).

FTIR experiments were performed with pellets prepared by pressing about 200 mg of catalyst powder (1 wt.%) diluted in KBr. Measurements were recorded on a Bruker Equinox 55 FTIR spectrometer at ambient temperature in the 4000–400 cm^{-1} range. Spectra were recorded with a resolution of 2 cm^{-1} and by co-addition of 64 scans. *In situ* DRIFT spectra were recorded on the same apparatus equipped with accessories for the diffuse reflectance and a room environment stainless steel manufactured by Harrick Scientific Corporation. A double thermocouple system can regulate the temperature inside the chamber and near the sample. The gaseous flow passing through the chamber is controlled by mass flow controllers. The pretreatment (350 °C for 4 h) and the catalytic test have been performed under the same conditions (gas flow rates, temperature ramp), but with 30 mg of pure sample. All spectra are presented in absorbance after subtracting the spectrum of the reference sample (KBr powder).

XRD measurements were performed by a Bruker D8 Advance diffractometer using CuK_α radiation ($\lambda = 1.5406$ Å) in the 2θ range 20–55°, with a step size of 0.02° and an integration time of 6 seconds.

Carbon black (CB) Printex U (from Evonik) was chosen as model for soot particles oxidation. Its chemical mass composition in percentage is: C = 92; H = 0.95; O = 4.4; N = 0.32 and S = 0.57. The specific area of the CB reaches 100 $m^2\ g^{-1}$ [17]. The CB–catalyst mixture was performed and prepared in loose contact conditions [1,18]. Six percent of CB and 94% of catalyst were introduced in a small flask and were simply shaken for 20 minutes. The catalytic test towards CB oxidation was studied by TG–DTA measurements. About 30 mg of CB–catalyst mixture were loaded in an alumina crucible and heated from room temperature to 650 °C (heating rate: 5 °C min^{-1}) in air flow (75 mL min^{-1}). TG–DTA results will be used to determine catalytic performances and CB oxidation rate.

The oxidation of toluene was carried out in a continuous flow reactor with a fixed bed at atmospheric pressure. Before each test, the catalyst (100 mg) was dried in air (2 L h^{-1}) at 500 °C (1 °C min^{-1}) for 4 h in order to remove the hydroxyl groups, water or moisture adsorbed on the catalyst and thus to activate it [19]. The feed gas reactant mixture was made of 1000 ppm of toluene and 10% O_2 in N_2 (total ow rate: 100 mL min^{-1}). After a stable feed, it passed through the catalyst and the temperature was increased from room temperature to 500 °C at a rate of 1 °C min^{-1}. Toluene conversion was checked in parallel using a CP–4900 μGC (Varian).

The simultaneous oxidation of toluene and CB was studied, considering 1000 ppm of toluene and 10% O_2 in N_2 passed through CB–catalyst mixture (100 mg of catalyst + 6% of CB).

The effect of the presence of NO_x (NO_2 + NO) in the feed gas (900 ppm) was also studied for the both different oxidations. The analysis of combustion products (NO_x, NO, NO_2, CO and CO_2) was obtained with Xentra 4900C continuous emissions analyzer (Servomex). Toluene conversion was checked using a CP–4900 μGC.

The volume hourly space velocity (VHSV), calculated at ambient temperature and atmospheric pressure, is 105,000 h^{-1}. Since the work was always carried out in the same reaction conditions (same toluene and/or NO_x flow and catalyst weight), the conversion values, which are directly comparable, were given.

3. Results and discussion

3.1. Effect of alkali metals on ZrO_2

The theoretical alkali metal content of 0.15 ratio molar in the catalysts was almost confirmed by ICP–MS. Indeed, the experimental molar ratio of the alkali metal in the samples was found to be slightly lower: 0.129 ± 0.015 (Table 1).

The specific area of the catalysts decreases with increasing temperature of calcination (Table 1). It decreases from 201 $m^2\ g^{-1}$ for ZrO_2 calcined at 300 °C to 84 $m^2\ g^{-1}$ for the same sample calcined at 600 °C. For the impregnated alkali samples before calcination, the specific area decreases when the molar mass of the alkali metal increases. It goes from 173 $m^2\ g^{-1}$ in the case of $Li_{0.15}/ZrO_2$ to 86 $m^2\ g^{-1}$ in the case of $Cs_{0.15}/ZrO_2$. The decrease of specific area can be attributed to the reorganization within the network of zirconia reducing the porosity of the solid [20]. After calcination at 600 °C, the specific surface of $Li_{0.15}/ZrO_2$ is four times (21 $m^2\ g^{-1}$) lower than the value of the support ZrO_2 (84 $m^2\ g^{-1}$). The addition of an alkali promoter leads to decrease markedly the specific surface of our catalysts. K and Na can migrate into the solid ZrO_2 and stabilize the tetragonal phase. Na promotes the good crystallization of the solid [20]. Other alkali metals (Li, Rb, Cs) facilitate the transformation of the tetragonal phase to the monoclinic phase. Indeed, the monoclinic phase (formed with Li, Cs) has a smaller surface area compared to the tetragonal phase, and then, the specific surface of the samples with Li and Cs is smaller than the value of the sample with Na.

A XRD study of ZrO_2 (calcined at 300 °C and 600 °C) and the different $alkali_{0.15}/ZrO_2$ catalysts calcined at 600 °C was carried out and the diffractograms obtained are displayed in Fig. 1. It shows that ZrO_2 calcined at 300 °C is an amorphous phase. The monoclinic phase (JCPDS 65.1023) appears significantly in the case of ZrO_2 calcined at 600 °C and $Li_{0.15}/ZrO_2$. For the tetragonal phase (JCPDS 50.1089), it is stabilized in the case of $Na_{0.15}/ZrO_2$, and less apparent in the case of $K_{0.15}/ZrO_2$. Indeed, according to Liu et al. [21], Na is able to diffuse inside the bulk of particles and stabilises the zirconia tetragonal phase. The tetragonal phase is predominant in the other catalysts. These results are in accordance with BET specific area results (Table 1).

DTA experiments (Fig. 2) of the different samples of $alkali_{0.15}/ZrO_2$ show the existence of exothermic peaks. These peaks are not accompanied by any significant mass loss (TG curves not shown). For the support calcined at 300 °C and the catalysts impregnated and dried at 115 °C, the first peak of crystallization of the tetragonal phase [16] is shifted to a higher temperature (428 °C in the case of the support and 433–600 °C in the case of promoted catalysts versus the molar mass of the alkali). Going from Li to Cs, the intensity of the first peak decreases; therefore the crystallization of amorphous ZrO_2 to tetragonal phase is inhibited. For the same type of preparation, the delay of crystallization increases when the molar mass of the alkali increases. A peak appears at high temperature (910 °C) in the case of $Na_{0.15}/ZrO_2$. It corresponds to the crystallization to monoclinic phase [22]. Indeed, the stability of the tetragonal phase (Fig. 1) can accelerate the appearance of monoclinic phase at this temperature. This observation is consistent with the observation of Liu et al. [22]. Thus, the presence of alkali metals on ZrO_2 calcined at 300 °C has an effect on the mode of crystallization of ZrO_2 during the calcination of catalyst up to 600 °C.

3.2. Impregnation of transition metals

The theoretical content of transition metals was confirmed by elemental analysis (Table 1). The molar ratio M/ZrO_2 was between 0.073 and 0.097. When the transition metal was impregnated alone or with a low amount of Cs, the molar ratio was between 0.086 and 0.097 molar ratio. The Cs/ZrO_2 molar ratio was 0.012. When the transition metal was impregnated with a high amount of Cs, the M/ZrO_2 molar ratio decreased to 0.073–0.074 and the corresponding Cs/ZrO_2 molar ratio was 0.094–0.1.

The impregnation of transition metal leads to materials with similar specific areas, comparable to that obtained from the support (in similar experimental conditions). The adding of a low amount of Cs leads also to the same

Table 1
Chemical composition of the catalysts calcined at 600 °C and specific areas of the catalysts before and after calcination at 600 °C.

Catalyst	Chemical composition			BET specific area ($m^2\ g^{-1}$)	
	Theoretical content (Alkali/ZrO_2 and/or M/ZrO_2, wt.%)	Experimental content (Alkali/ZrO_2 and/or M/ZrO_2, wt.%)	Corresponding experimental molar ratio	Before calcination	After calcination at 600 °C for 4 h
ZrO_2	–	–	–	201	84
$Li_{0.15}/ZrO_2$	0.845	0.813	0.144	173	21
$Na_{0.15}/ZrO_2$	2.819	2.433	0.129	156	34
$K_{0.15}/ZrO_2$	4.809	3.660	0.114	134	34
$Rb_{0.15}/ZrO_2$	10.250	8.351	0.122	107	27
$Cs_{0.15}/ZrO_2$	16.235	14.210	0.131	86	21
$Cs_{0.15}–Co_{0.1}/ZrO_2$	16.235 (Cs) 4.783 (Co)	10.198 (Cs) 3.505 (Co)	0.094 (Cs) 0.073 (Co)	85	17
$Cs_{0.015}–Co_{0.1}/ZrO_2$	1.623 (Cs) 4.783 (Co)	1.346 (Cs) 4.229 (Co)	0.012 (Cs) 0.088 (Co)	204	68
$Co_{0.1}/ZrO_2$	4.783	4.119	0.086	192	95
$Cs_{0.15}–Cu_{0.1}/ZrO_2$	16.235 (Cs) 5.153 (Cu)	10.834 (Cs) 3.797 (Cu)	0.100 (Cs) 0.074 (Cu)	83	12
$Cs_{0.015}–Cu_{0.1}/ZrO_2$	1.623 (Cs) 5.153 (Cu)	1.260 (Cs) 5.014 (Cu)	0.012 (Cs) 0.097 (Cu)	196	96
$Cu_{0.1}/ZrO_2$	5.153	4.452	0.086	199	90

observations, but in the case of the impregnation of Cu or Co with a high amount of Cs, the specific areas of corresponding catalysts are similar to those obtained from $Cs_{0.15}/ZrO_2$ (in similar experimental conditions).

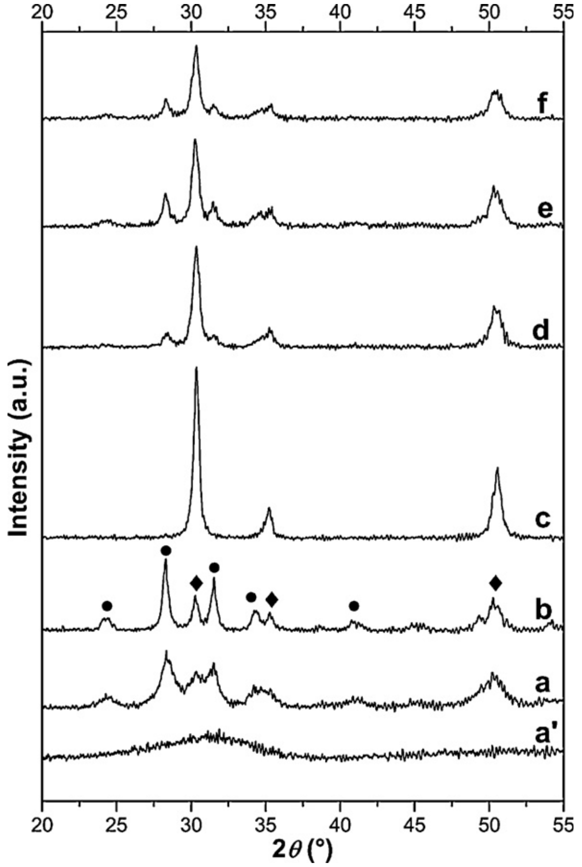

Fig. 1. XRD patterns of ZrO_2 (a': calcined at 300 °C, a: calcined at 600 °C) and catalysts calcined at 600 °C (b: $Li_{0.15}/ZrO_2$, c: $Na_{0.15}/ZrO_2$, d: $K_{0.15}/ZrO_2$, e: $Rb_{0.15}/ZrO_2$, f: $Cs_{0.15}/ZrO_2$); (•) monoclinic phase; (◆) tetragonal phase.

A XRD study of $Cs_x–M_{0.1}/ZrO_2$ catalysts calcined at 600 °C was carried out and the obtained diffractograms are displayed in Fig. 3. For copper based catalysts (Fig. 3A), there is a stabilization of the tetragonal phase with all catalysts, but for the CuO phase ($2\theta = 38.8$), CuO lines are observed (JCPDS 48.1484) in the presence of the alkali metal ($Cs_{0.15}–Cu_{0.1}/ZrO_2$). The same phenomenon was

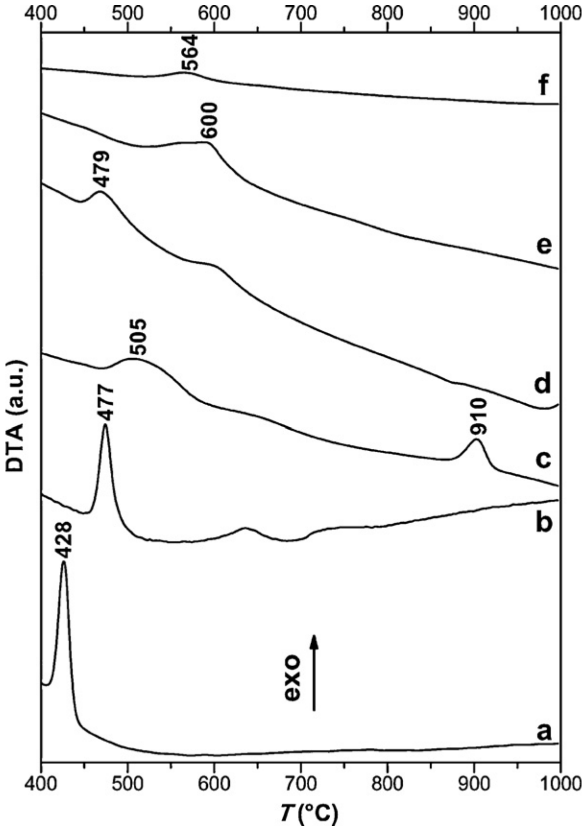

Fig. 2. DTA curves of ZrO_2 calcined at 300 °C (a: and dried solids, b: $Li_{0.15}/ZrO_2$, c: $Na_{0.15}/ZrO_2$, d: $K_{0.15}/ZrO_2$, e: $Rb_{0.15}/ZrO_2$, f: $Cs_{0.15}/ZrO_2$).

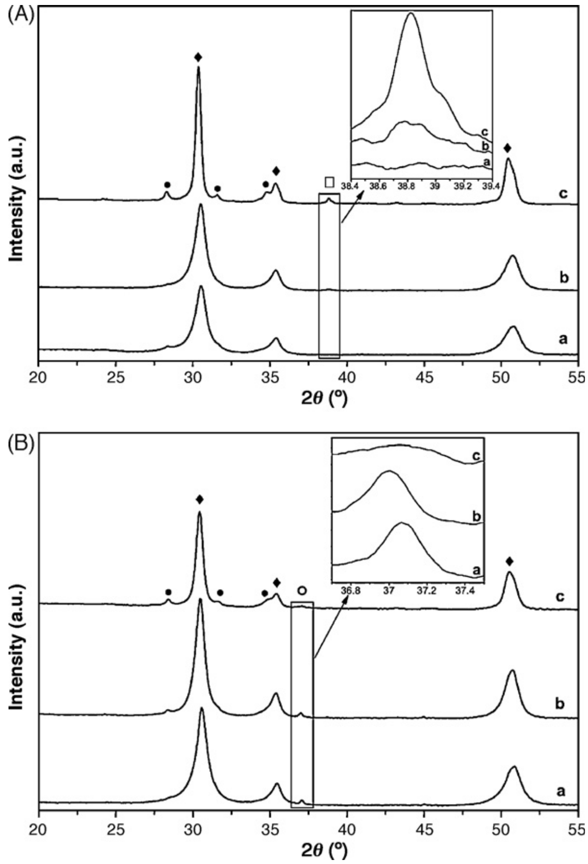

Fig. 3. XRD patterns of Cs_x–$M_{0.1}ZrO_2$ (A: copper based catalysts, B: cobalt based catalysts) calcined at 600 °C (a: $M_{0.1}/ZrO_2$, b: $Cs_{0.015}$–$M_{0.1}/ZrO_2$, c: $Cs_{0.15}$–$M_{0.1}/ZrO_2$); (•) monoclinic phase; (◆) tetragonal phase, (□) CuO phase, (°) Co_3O_4 cubic phase.

observed by Lick et al. [23]. Thus, the alkali metal allows the formation of the CuO phase and should influence the Cu segregation, leading to observable crystals with the XRD technique [23]. For catalysts with cobalt (Fig. 3B), in the absence of Cs or in its presence with a low amount, there is a line (at $2\theta = 37.09$) corresponding to Co_3O_4 (JCPDS 42.1467). The absence of a Co oxide phase peak in the XRD pattern for the $Cs_{0.15}$–$Co_{0.1}/ZrO_2$ sample shows that the oxide particles must be finely dispersed as amorphous or small sized (size < 3 nm) particles invisible by XRD [14]. Park et al. [24] demonstrated that the characteristic lines of Co_3O_4 are shown only with Na/Co $\leq$ 0.015 (atomic ratio) and for samples with Na/Co $\geq$ 0.03, characteristic peaks of β-$Na_{0.6}CoO_2$ increase with increasing Na content.

3.3. Oxidation tests

3.3.1. Catalytic oxidation of carbon black

Catalytic performance in CB oxidation was determined by the use of DTA–TG curves. The maximum of the curve corresponds to the temperature of the highest rate of CB oxidation T_{max} (Fig. 4). The oxidation of CB with ZrO_2 alone is between 414 and 617 °C with a maximum CB oxidation rate (975 $\mu g\ s^{-1}\ g^{-1}{}_{CB}$) at $T_{max} = 575$ °C. A shift to lower T_{max} occurs in the presence of catalysts promoted with alkali, especially for $Cs_{0.15}/ZrO_2$ ($T_{max} = 355$ °C). The oxidation rate goes from 1966 $\mu g\ s^{-1}\ g^{-1}{}_{CB}$ with $Li_{0.15}/ZrO_2$ to 2516 $\mu g\ s^{-1}\ g^{-1}{}_{CB}$ with $Cs_{0.15}/ZrO_2$. The higher performance of Cs-loaded catalyst for soot ignition cannot be explained by the specific area [25]. The results show that the use of alkali-impregnated catalyst is beneficial for the oxidation of CB, reaching the best results with the "heavier" alkali. The addition of transition metals (especially Cu), provided for the enhancement of toluene

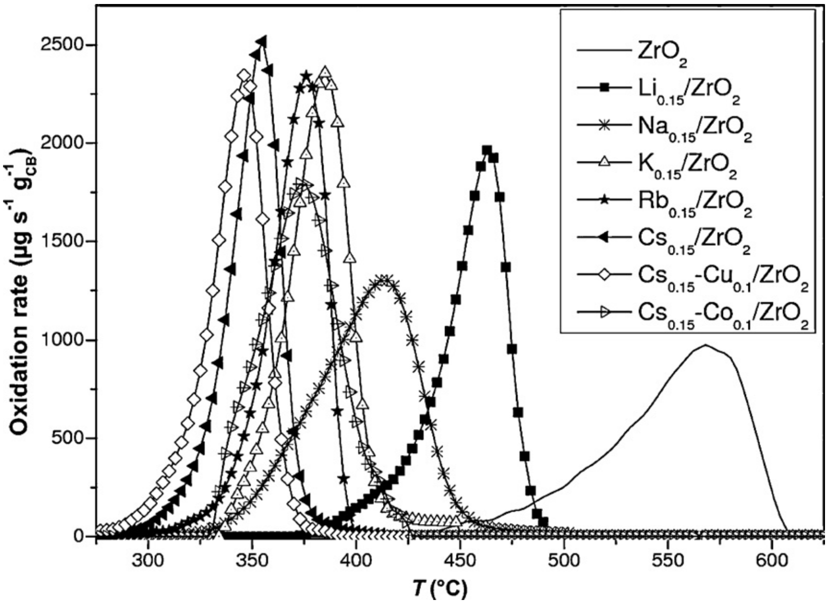

Fig. 4. CB oxidation vs. reaction temperature.

oxidation, is also interesting for the oxidation of CB. However, for Co based catalyst ($Cs_{0.15}$–$Co_{0.1}/ZrO_2$), T_{max} value is lower than for $Cs_{0.15}/ZrO_2$. For the catalyst impregnated by Cu and Cs, the CB oxidation rate reaches a maximum value of 2346 μg s^{-1} g^{-1}_{CB} and at T_{max} (347 °C), slightly lower than that achieved with $Cs_{0.15}/ZrO_2$. These experiments suggest a synergistic effect between the alkali metal and Cu already observed in a previous work [11]. The alkali metal promoter interacts with the supported copper(II) species and favours their participation following a redox mechanism. It is assumed that the formation of CuO phase, under the form of large or small particles, is responsible for this activity enhancement, CuO species being more active than isolated copper and copper clusters for CB oxidation reaction [26]. The performance of CuO based catalysts in the CB oxidation has been also attributed to the high mobility of the copper ions during burn-off [27]. Moreover, it was shown in the study of Laversin et al. [11] that the alkali promoters are species that not only favour CB–catalyst contact, but also enhance the participation of active oxygen from copper oxide and oxide carrier to oxidize CB. Furthermore, in the case of $Cs_{0.015}$–$Cu_{0.1}/ZrO_2$ and $Cu_{0.1}/ZrO_2$, the maximum CB oxidation rate is lower than those for the catalysts: $Cs_{0.15}/ZrO_2$ and $Cs_{0.15}$–$Cu_{0.1}/ZrO_2$. Moreover, T_{max} of these catalysts is also the highest among all the catalysts. This shows the contribution of Cs in the oxidation of carbonaceous particles. In fact, the presence of alkali metals favours contact between the catalyst and CB and enhances the catalyst's ability to release active oxygen species. Moreover, the presence of higher alkali content induces further activity improvement [11]. The XRD results (Fig. 3A) show that in the presence of high amount of Cs, the CuO phase appears on the XRD patterns. T_{max} found for $Cs_{0.15}$–$Cu_{0.1}/ZrO_2$ catalyst is lower than those of $Cs_{0.015}$–$Cu_{0.1}/ZrO_2$ and $Cu_{0.1}/ZrO_2$ catalysts. This suggests that the activity can be associated mainly with Cs and with the wetting effect of the catalytic surface that this metal confers. Cs- and Cu-based catalysts will then be used in the others tests of CB oxidation.

3.3.2. Catalytic oxidation of toluene

The behaviour of the different catalysts for the toluene oxidation is presented in Fig. 5 and Table 2. For the catalysts promoted by alkali alone, the oxidation of toluene is only complete at 500 °C for the best catalyst $Cs_{0.15}/ZrO_2$. Cobalt or copper impregnation on $Cs_{0.15}/ZrO_2$ leads to powerful catalysts, especially for $Cs_{0.15}$–$Co_{0.1}/ZrO_2$. Moreover, the solid with a low amount of Cs ($Cs_{0.015}$–$Co_{0.1}/ZrO_2$) allows us to reach a $T_{50\%}$[1] = 296 °C instead of $T_{50\%}$ = 371 °C for $Cs_{0.15}$–$Co_{0.1}/ZrO_2$ (Table 2). Moreover, cobalt impregnation alone on ZrO_2 presents also a good performance, similar to $Cs_{0.015}$–$Co_{0.1}/ZrO_2$ for toluene oxidation. Indeed, the presence of Co_3O_4 phase in Co based catalysts leads to improve toluene conversion to CO_2 [13,14]. This Co_3O_4 phase is observable in our catalysts (Fig. 3B). The catalytic performance of $Cs_{0.15}$–$Co_{0.1}/ZrO_2$ is lower than that of the same sample without, or with a low amount, of Cs. Therefore, the presence of high amount of alkali metal decreases the activity of the Co_3O_4 phase for the toluene oxidation. The good performance of cobalt-impregnated catalyst should be due to dispersed species of cobalt. Thus, it seems that the amount of reducible species plays a non-negligible role in the catalytic properties in oxidation reactions. The higher the amount of reducible species in the temperature range of catalytic activity is, the better the catalytic performance [19]. The good performance of Co based catalysts in comparison with Cs based catalysts for toluene oxidation could be due to the easier reducibility of Co_3O_4 compared to Cs_2O. In fact, Co shows reduction peaks in the temperature range 100–400 °C [14,19], although Cs shows a maximum reduction temperature pointed out at 520 °C [1]. One reason for the lower performance of Cs high amount catalyst is the possible formation of a Cs–Co phase. Thus, the XRD results (Fig. 3B) show that the Co_3O_4 phase formation is diminished in the presence of high amount of Cs.

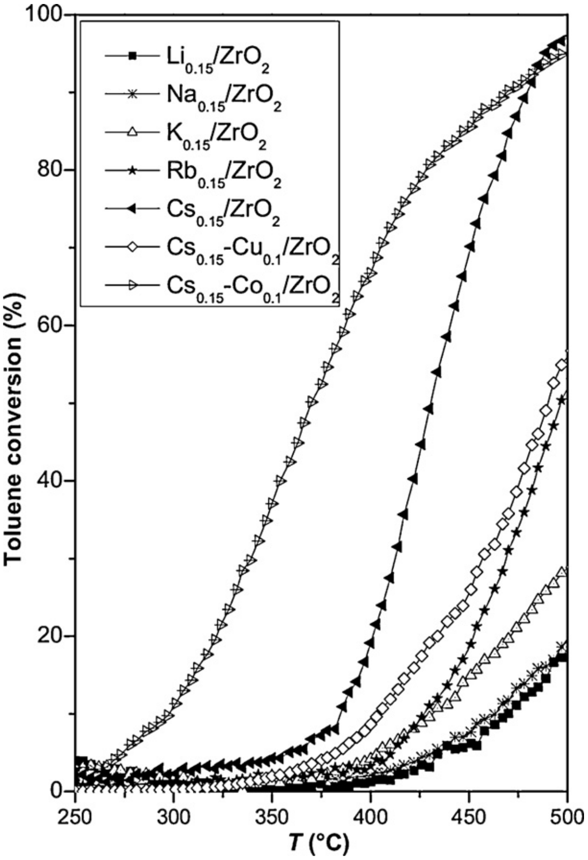

Fig. 5. Toluene conversion vs. reaction temperature.

3.3.3. Catalytic removal of CB in the presence of toluene or NO_x

3.3.3.1. Oxidation of carbon black in the presence of toluene. For comparison reasons, the tests of CB oxidation were all recorded in the same conditions by the use of a microreactor (Table 3). The ignition temperature T_i for CB oxidation was determined as light-off temperature, at

---

[1] Temperature at which 50% of toluene is oxidized.

Table 2
Toluene oxidation and NO_x conversion values.

Catalyst	$T_{50\ \%}$ and (T_i) values for toluene oxidation (°C)			Maximum of NO_x conversion (%)
	Toluene + O_2	Toluene + O_2 + CB	Toluene + O_2 + NO	
$Cs_{0.15}/ZrO_2$	443 (283)	451 (276)	490 (308)	14.9 (at 430 °C)
$Cs_{0.15}$–$Cu_{0.1}/ZrO_2$	487 (300)	-	-	-
$Cs_{0.15}$–$Co_{0.1}/ZrO_2$	371 (260)	423 (220)	399 (250)	Not observable
$Cs_{0.015}$–$Co_{0.1}/ZrO_2$	296 (260)	269 (208)	279 (210)	22.9 (at 293 °C)
$Co_{0.1}/ZrO_2$	294 (260)	285 (193)	285 (220)	64.1 (at 300 °C)

Table 3
CB oxidation and NO_x conversion values.

Catalyst	T_{max} and (T_i) for CB oxidation (°C)			Maximum of NO_x conversion (%)
	CB + O_2	CB + O_2 + toluene	CB + O_2 + NO	
$Cs_{0.15}/ZrO_2$	349 (275)	325 (235)	323 (270)	22.6 (340–450 °C)
$Cs_{0.15}$–$Cu_{0.1}/ZrO_2$	321 (268)	308 (239)	355 (255)	25.9 (at 370 °C)
$Cs_{0.015}$–$Cu_{0.1}/ZrO_2$	496 (362)	451 (410)	384 (291)	22.6 (at 390 °C)
$Cu_{0.1}/ZrO_2$	498 (335)	497 (329)	405 (200)	16.3 (at 410 °C)

which a significant evolution of CO_2 started. In a previous study [28], Aouad et al. showed that the presence of propene in reactant gases flow was shown to be beneficial to CB elimination in the presence of Ru_xCe catalysts, knowing that the temperature of total oxidation of propene is lower than that of CB (NC 330, Evonik). In this work, the tests were performed with toluene and CB (Printex U). For all the catalysts, a decrease between 10–20 °C of T_i and T_{max} is recorded for CB oxidation in the presence of toluene in comparison with simple CB oxidation. Thus, the presence of the hydrocarbon in the reactant gases mixtures is not only beneficial to the oxidation of a part of CB at low temperatures but also to the faster oxidation of CB [28]. The exothermic effect of the toluene oxidation and/or toluene adsorption on CB can explain this enhancement. However, the toluene oxidation seems not to be improved by the CB oxidation. The CB oxidation is enhanced in the presence of toluene but

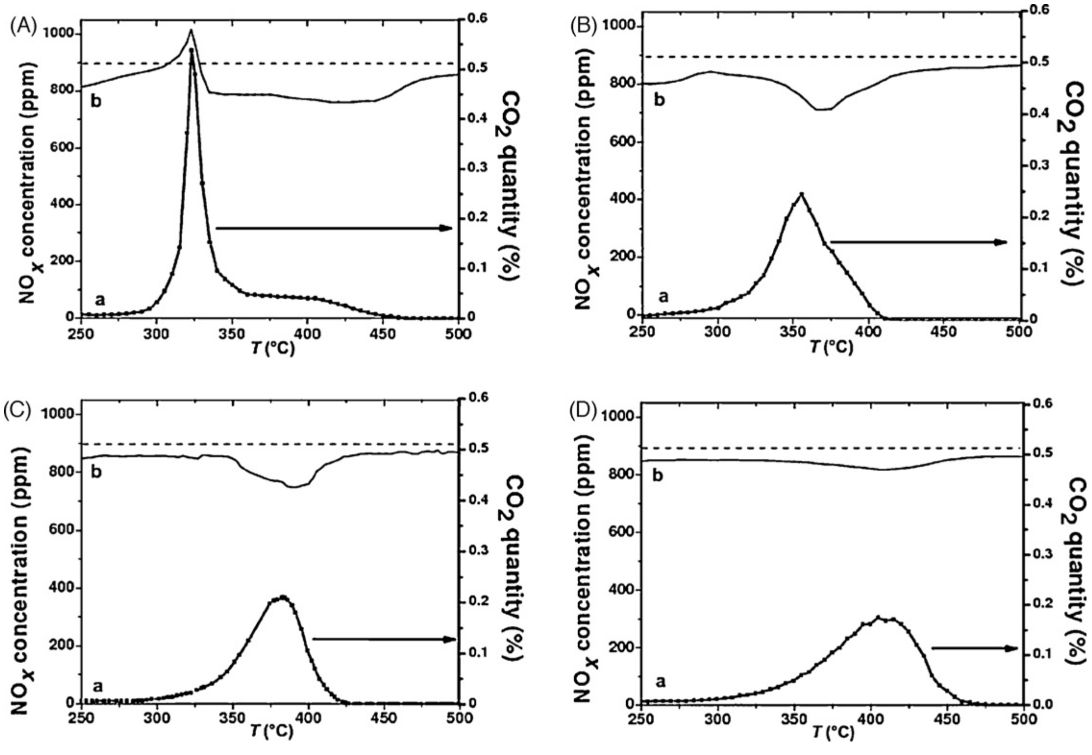

Fig. 6. Oxidation of CB vs. reaction temperature with the catalysts (A: $Cs_{0.15}/ZrO_2$, B: $Cs_{0.15}$–$Cu_{0.1}/ZrO_2$, C: $Cs_{0.015}$–$Cu_{0.1}/ZrO_2$, D: $Cu_{0.1}/ZrO_2$) in the presence of NO_x (a: CO_2 quantity of CB oxidation, b: NO_x concentration).

especially for the catalysts with a high amount of Cs ($Cs_{0.15}/ZrO_2$ and $Cs_{0.15}–Cu_{0.1}/ZrO_2$). However, the catalyst $Cs_{0.15}–Cu_{0.1}/ZrO_2$ is the best one. This can be attributed to the both participation of a high content of alkali metal and CuO phase.

3.3.3.2. Oxidation of carbon black in the presence of NO_x. The results concerning the CB oxidation in the presence of NO_x are shown in Table 3 and Fig. 6. Dotted lines in the figure represent the NO_x concentration in the gas feed in the presence of 10% O_2, i.e., the points below and above this line mean the occurrence of NO_x sorption/reduction and NO_x desorption respectively. For the sample $Cs_{0.15}/ZrO_2$, T_i of CB oxidation in the presence of NO_x is slightly enhanced compared to that in the test of CB oxidation alone, but lower than that in presence of toluene. The same phenomenon is recorded for the values of T_{max}. An increase of NO_x is also observable. $Cs_{0.15}/ZrO_2$ exhibits sorptive NO_x, which is followed by a broad NO_x desorption at higher temperatures. It gives rise to a sharp NO_x desorption, which starts before the beginning of CO_2 evolution. Unlike the case of the catalyst alone (not shown), very sharp and

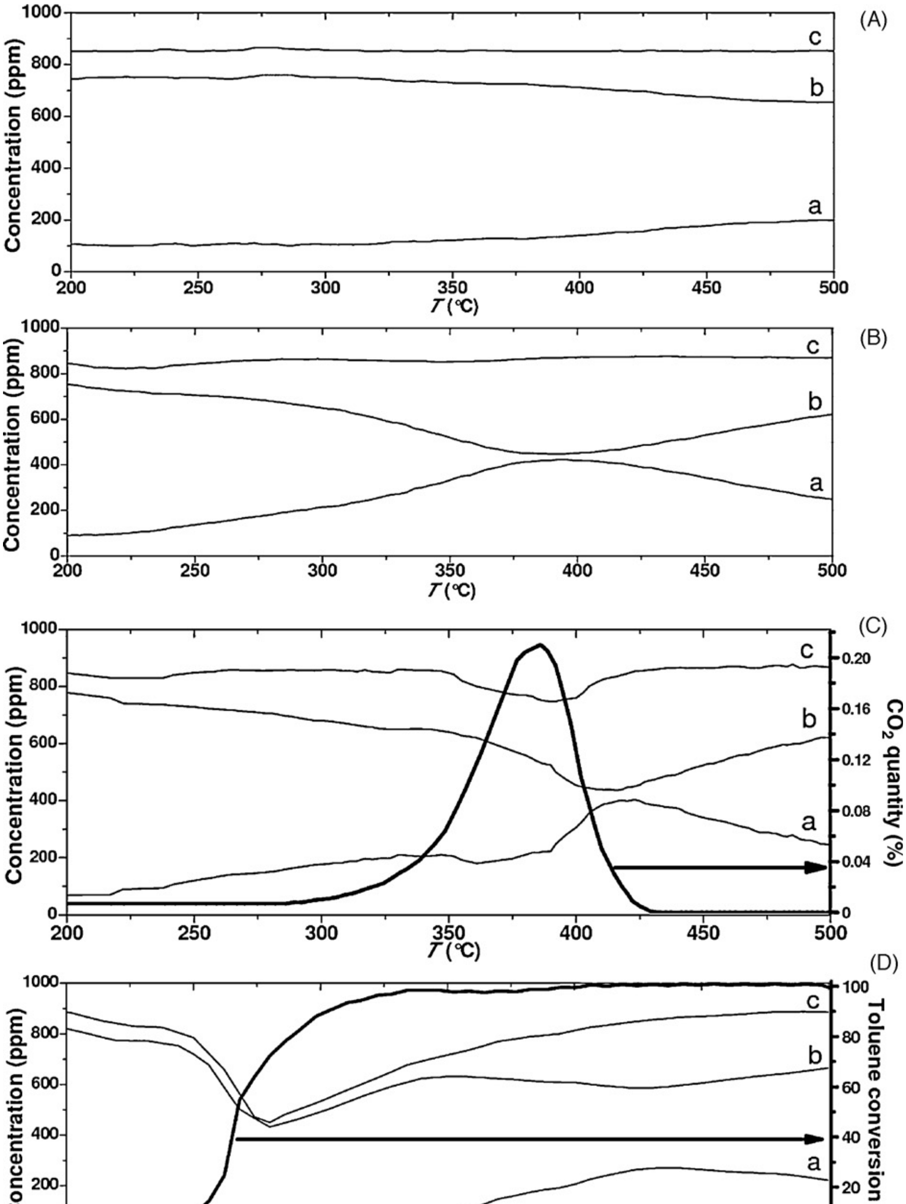

Fig. 7. Effect of the presence of catalyst ($Cs_{0.015}–Cu_{0.1}/ZrO_2$) and reducer (CB or toluene) in the conversion of NO_x and the oxidation of NO (A: without catalyst, B: with catalyst, C: with catalyst in the presence of CB, D: with catalyst in the presence of toluene, a: NO_2, b: NO, c: NO_x).

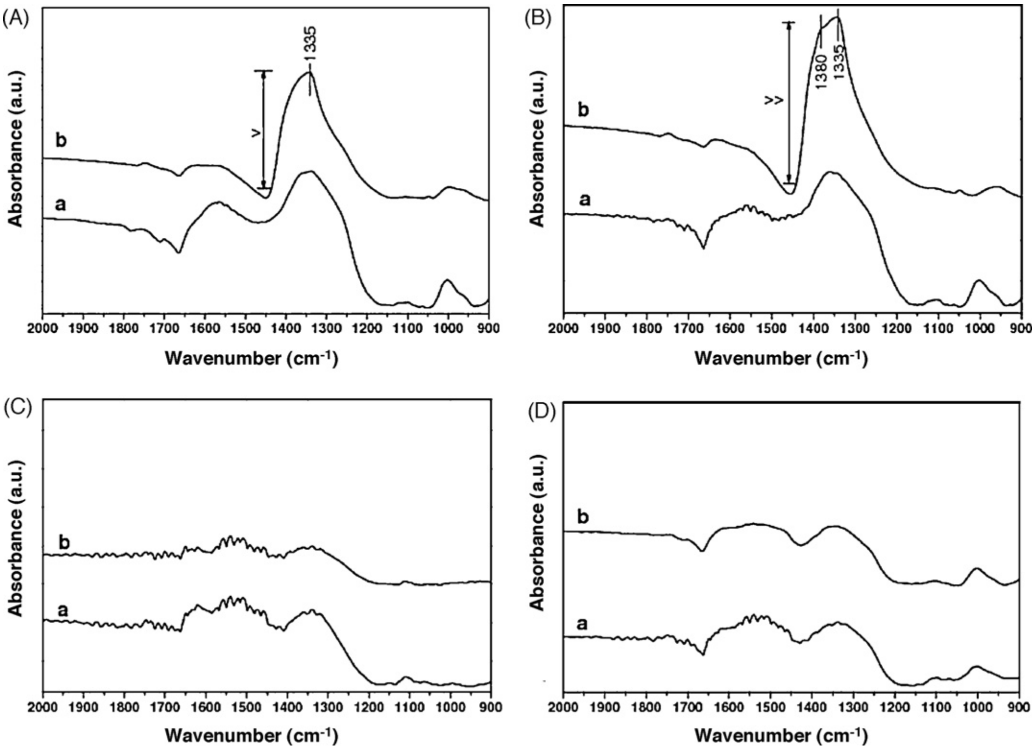

Fig. 8. Infrared spectra of the catalysts (A: $Cs_{0.15}/ZrO_2$, B: $Cs_{0.15}–Cu_{0.1}/ZrO_2$, C: $Cs_{0.015}–Cu_{0.1}/ZrO_2$, D: $Cu_{0.1}/ZrO_2$) after test (a: CB + O_2, b: CB + O_2 + NO).

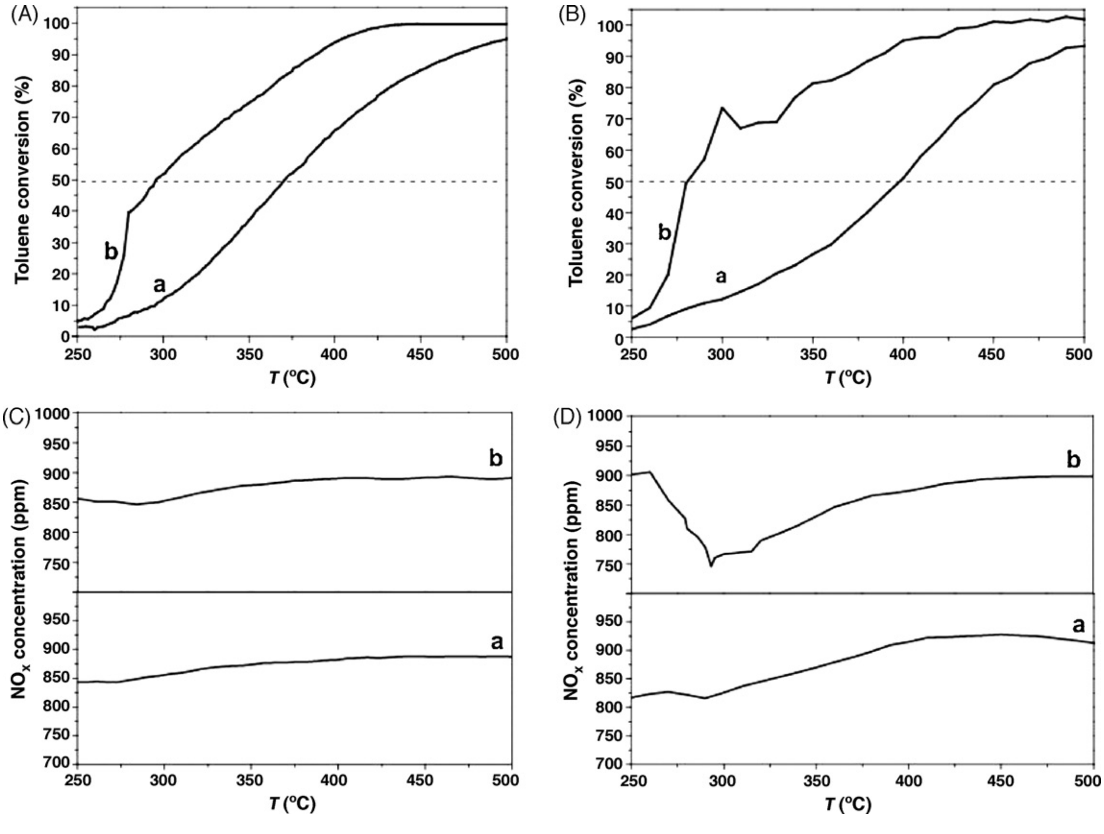

Fig. 9. Toluene conversion and NO_x concentration vs. reaction temperature on the catalysts (a: $Cs_{0.15}–Co_{0.1}/ZrO_2$, b: $Cs_{0.015}–Co_{0.1}/ZrO_2$) (A: toluene conversion without NO_x, B: toluene conversion with NO_x, C: NO_x concentration without toluene, D: NO_x concentration with toluene).

temporary desorption of NO_x appears at 323 °C (also T_{max} of CB oxidation). After this, the NO_x concentration drops suddenly below the inlet level suggesting the occurrence of reactions between NO and CB [25] in the temperature range 323–450 °C. This is consistent with a larger area below the dotted line than that above the line (Fig. 6A). This phenomenon is in accordance with the observation of Ito et al. [25]. First, a sharp desorption of NO_x should result from a very fast and local exotherm due to soot ignition. As described above, the temperature of soot ignition is lowered when a large amount of NO is pre-adsorbed on the catalysts. If soot would directly be reacted with desorbed NO_x, the ignition must be observed after the beginning of NO_x desorption. However, this is not the case. This leads to another important suggestion that soot ignition is presumably promoted by adsorbed NO_x species [25]. For $Cs_{0.15}$–$Cu_{0.1}/ZrO_2$, T_{max} of CB oxidation is less good; it rises from 321 °C to 355 °C, but a conversion of NO_x is detected at 370 °C, which is close to the maximum CB oxidation rate. The presence of NO_x is unfavourable for toluene oxidation with this catalyst although this catalyst records the high NO_x conversion. For $Cs_{0.015}$–$Cu_{0.1}/ZrO_2$, T_i and T_{max} of CB oxidation are considerably enhanced. A decrease of about 110° is observed for T_{max} and 70° for T_i. A good NO_x conversion is recorded with this catalyst. In the case of the catalyst $Cu_{0.1}/ZrO_2$, the CB oxidation is enhanced with a shift to a lower temperature in the presence of NO_x (Table 3), but there is a low NO_x conversion for $Cu_{0.1}/ZrO_2$ compared to $Cs_{0.015}$–$Cu_{0.1}/ZrO_2$. As described on Fig. 6, the ignition temperature is lowered when a large amount of NO_x is pre-adsorbed on these catalysts. If the CB directly reacts with desorbed NO_x, the ignition must be observed after the beginning of NO_x desorption. The addition of Cs not only activates CB ignition, but also increases NO_x adsorption, which is also effective for CB ignition [25].

Fig. 8 shows the infrared spectra after CB oxidation tests without (spectra (a)) and in the presence of NO_x (spectra (b)). The NO_x sorption leads to the formation of bidentate and/or monodentate nitrates species on the surface. Two bands at 1380 and 1335 cm^{-1} are detected after tests in the presence of NO_x for $Cs_{0.15}/ZrO_2$ and $Cs_{0.15}$–$Cu_{0.1}/ZrO_2$. These bands are attributed to free NO_3^- groups (1380 cm^{-1}) and to monodentate NO_3^- groups (1335 cm^{-1}) [1]. Presence of bridged NO_3^- groups could not be excluded; their characteristic band (~1620 cm^{-1}) could be masked by adsorbed water band [1]. The amount of nitrate is large for the catalyst $Cs_{0.15}$–$Cu_{0.1}/ZrO_2$ and lower for $Cs_{0.15}/ZrO_2$. For the samples $Cs_{0.015}$–$Cu_{0.1}/ZrO_2$ and $Cu_{0.1}/ZrO_2$, there is not any significant adsorption. The large amount of nitrate adsorbed in the case of $Cs_{0.15}/ZrO_2$ and $Cs_{0.15}$–$Cu_{0.1}/ZrO_2$ is due to the strong basicity of Cs. The oxidative adsorption of NO was also increased to form nitrate on the solid surface [25]. The use of a low amount of Cs impregnated with Cu, leads to a great shift of T_i and T_{max} of CB oxidation to a low range of temperatures. The catalysts Cs_x–$Cu_{0.1}/ZrO_2$ possess the combination of NO_x–oxidation activity and moderate basicity, yielding in significant synergism in the oxidative adsorption as to yield nitrite (NO_2^-) and/or nitrate (NO_3^-) on the surface.

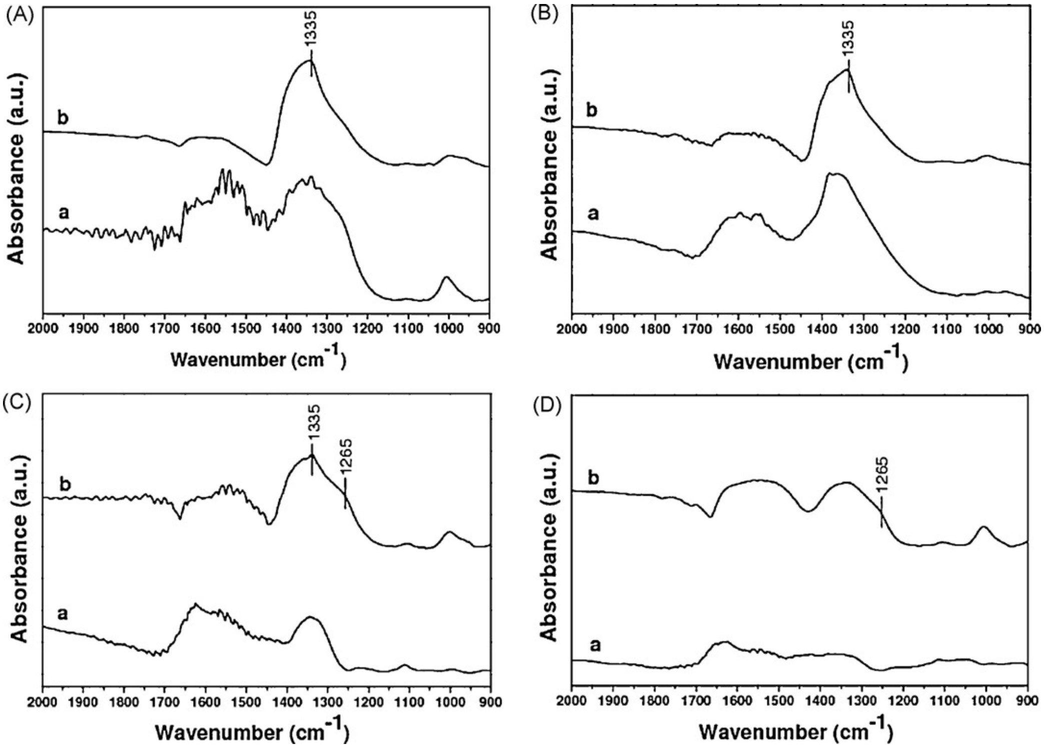

Fig. 10. Infrared spectra of different catalysts (A: $Cs_{0.15}/ZrO_2$, B: $Cs_{0.15}$–$Co_{0.1}/ZrO_2$, C: $Cs_{0.015}$–$Co_{0.1}/ZrO_2$, D: $Co_{0.1}/ZrO_2$) after tests: (a: toluene + O_2, b: toluene + O_2 + NO).

This explains the high NO_x conversion in the case of these catalysts, compared to $Cs_{0.15}/ZrO_2$ or $Cu_{0.1}/ZrO_2$. The maximum NO_x conversion corresponds to T_{max} of CB oxidation (Table 3). Comparing the curves of NO_x in the absence of CB (Fig. 7B) and in the presence of CB (Fig. 7C), the NO_x conversion is just observed when a maximum of CB is oxidized at T_{max}. This conversion is accompanied with a decrease of NO_2 quantity (curve a). Thus, NO_2 participates in the CB oxidation. This is explained by the need for NO_2 as an intermediate for the catalyst to work efficiently [6], especially in the oxidation of CB [29]. The detailed mechanism of CB–NO_x interaction is not clear at this stage, but this may be explained by considering adsorbed nitrate species as an oxidizing agent [25]. The oxidation of NO to the nitrate is supposed to proceed in two steps: [15]

$$NO + \frac{1}{2}O_2 \rightarrow NO_2 \quad (1)$$

$$2NO_2 + O^{2-} \rightarrow 2NO_3^- \quad (2)$$

where O^{2-} means lattice oxygen in oxides. Reaction (1) is the essential step to form the nitrate ion; thus, the high activity of the oxidation catalyst is important for the first step. If the oxidation activity is insufficient, adsorption of NO_x as nitrate ion, NO and NO_2 species, proceeds. The second step (reaction (2)) also depends strongly on the kind of the catalyst [15]. The reaction (1) is a simple catalytic oxidation (Fig. 6B), whereas the reaction (2) is oxidative NO_x uptake in a sorbent [15]. The formed nitrate ions are stored on the surface and/or in the bulk of zirconia [15].

3.3.4. *Catalytic oxidation of toluene in the presence of CB or NO_x*

3.3.4.1. Oxidation of toluene in the presence of CB. The results of comparison between toluene oxidation alone and toluene oxidation in the presence of CB are summarized on Table 2. T_i of toluene oxidation is determined when a significant toluene conversion started. For $Cs_{0.15}/ZrO_2$, $T_{50\%}$ of toluene conversion is less good in the presence of CB, but T_i is slightly enhanced. This is due to the oxidation of CB proceeding before that of toluene oxidation. The same result is obtained with $Cs_{0.15}$–$Co_{0.1}/ZrO_2$. For $Cs_{0.015}$–$Co_{0.1}/ZrO_2$ and $Co_{0.1}/ZrO_2$, $T_{50\%}$ and T_i are both enhanced in the presence of CB. In this case, adsorption of toluene on CB should be important. The results show the interest of adding a low amount of alkali metal to cobalt in comparison with the simple catalyst $Co_{0.1}/ZrO_2$.

3.3.4.2. Oxidation of toluene in the presence of NO_x. The oxidation of toluene in the presence of NO_x is presented in Fig. 9 and Table 2. For $Cs_{0.15}/ZrO_2$, T_i and $T_{50\%}$ of toluene oxidation decrease in the presence of NO_x. The addition of Co to $Cs_{0.15}/ZrO_2$ enhances toluene oxidation, but not enough to reach the conversion obtained without NO_x. The low NO_x concentration observed at low temperatures (Table 2) should be due mainly to the adsorption of NO_x species by the catalyst with a alkali amount, by the formation of nitrates [15]. The diminution of the amount of Cs leads to enhance the performance, greatly for NO_x conversion and slightly for toluene oxidation compared to the same oxidation without presence of NO_x. $Co_{0.1}/ZrO_2$ catalyst allows us to enhance NO_x conversion in comparison with $Cs_{0.015}$–$Co_{0.1}/ZrO_2$, but the oxidation of toluene is more efficient in the presence of NO_x over the $Cs_{0.015}$–$Co_{0.1}/ZrO_2$ catalyst. Moreover, on Fig. 9B (b), toluene oxidation increases when the concentration of NO_x reaches its minimum. Therefore, the adding of a low amount of Cs to cobalt based catalysts leads to enhance toluene oxidation.

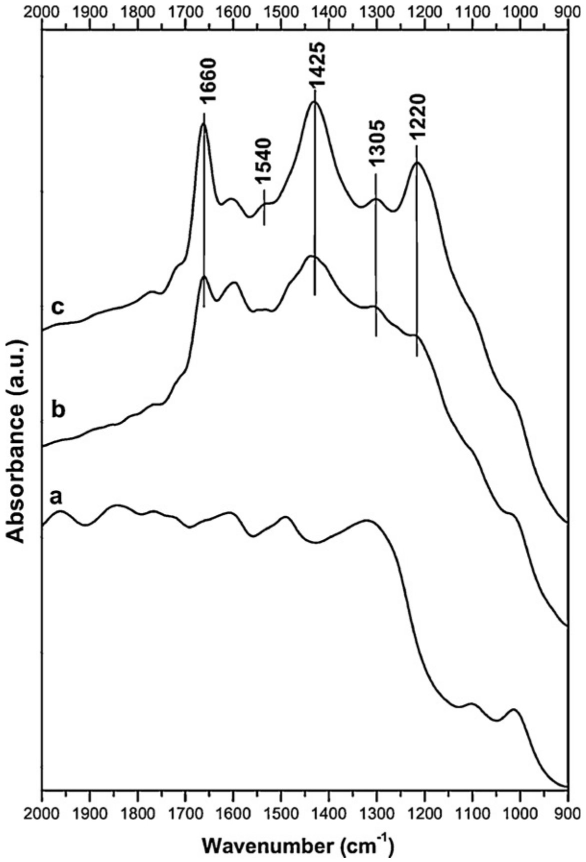

Fig. 11. *In situ* infrared spectra of $Cs_{0.015}$–$Co_{0.1}/ZrO_2$ at 350 °C (a: pretreatment under air flow, b: toluene + O_2, c: toluene + O_2 + NO).

FTIR measurements for catalysts tested (Fig. 10) are carried after simple toluene oxidation at 500 °C (spectra (a)) and after oxidation of toluene in the presence of NO_x (spectra (b)). For Cs based catalysts, a band at 1335 cm^{-1} corresponding to monodentate NO_3^- [1] is observed for the tests of toluene oxidation in the presence of NO_x. So, the catalysts with the higher alkali content show the presence of a strong absorbance band ascribed to monodentate NO_3^- species (1335 cm^{-1}). Therefore, NO_x could be stored as nitrate species on catalysts with higher alkali content. This phenomenon is in good agreement with previous works revealing the strong interaction of NO_x over alkali containing catalysts [1]. In this case, active oxidation sites of toluene could be occupied by NO_x. This could explain the lower performance of Cs high amount catalysts. On the contrary, nitrite species (1265 cm^{-1}) band showed in the case of $Cs_{0.015}$–$Co_{0.1}/ZrO_2$ and $Co_{0.1}/ZrO_2$ catalysts demonstrates that the transition metals have the ability to form NO_2 which is a stronger oxidizer than O_2 [23].

3.4. Operando DRIFT study

Fig. 11 shows *in situ* FT–IR spectra of $Cs_{0.015}$–$Co_{0.1}$/ZrO_2 at 350 °C. When introducing toluene and O_2, there are bands at 1660 and 1425 cm^{-1} corresponding to substituted aromatic compounds, a band at 1305 cm^{-1} corresponding to skeletal C–C stretching vibration and a band at 1220 cm^{-1} corresponding to carbon single bonded oxygen stretching. In the presence of NO in the gas mixture (toluene + O_2 + NO), the bands at 1660, 1425 and 1220 cm^{-1} are more intense and a band at 1540 cm^{-1} corresponding to R–NO_2 appears. Thus, the toluene oxidation is observed by the strong bands for aromatic substitutes, especially for the experiment with NO_x.

4. Conclusion

In this work, the catalytic performance of both oxidation of toluene and soot by alkali/ZrO_2 is found to increase in the following order: $Li_{0.15}/ZrO_2 \approx Na_{0.15}/ZrO_2 < K_{0.15}/ZrO_2 < Rb_{0.15}/ZrO_2 < Cs_{0.15}/ZrO_2$.

Catalysts impregnated by Co and Cs are active in the oxidation of toluene, whereas the catalysts based on Cu are more active in CB oxidation due to the active of CuO phase. Moreover, the contribution of cesium can enhance the participation of active oxygen from copper oxide to oxidize CB. In the case of the simultaneous oxidation of CB and toluene, the presence of VOCs enhances the oxidation of CB through the exothermic effect of VOCs oxidation. The catalyst impregnated with Cs and Cu is the most active one for CB oxidation alone or in the presence of toluene.

The presence of NO_x is favourable for the oxidation of toluene and CB. For the CB oxidation, a significant decrease of CB oxidation temperature in the presence of NO_x is obtained with $Cs_{0.015}$–$Cu_{0.1}$/ZrO_2. Due to the strong basicity of Cs, the oxidative adsorption of NO_x is increased to form nitrate on the solid surface. The CB combustion over such NO_x-sorbing catalysts is further accelerated, suggesting the occurrence of the NO_x–CB interaction on the catalyst surface. Adsorbed nitrate species are considered as oxidizing agents to promote CB ignition. The addition of Cs helps the activation of CB ignition, but also increases NO_x adsorption, which is also effective for CB ignition.

For toluene oxidation, $Cs_{0.015}$–$Co_{0.1}$/ZrO_2 is the best catalyst for toluene oxidation in the presence of CB or in the presence of NO_x.

Thus, our catalysts show good performances in the both simple and simultaneous removal of VOCs or CB in the presence of NO_x.

Acknowledgements

The "Nord-Pas de Calais" Region, the "Syndicat Mixte de la Côte d'Opale" and European Union via Interreg IV "Redugaz project" are gratefully acknowledged for financial support.

References

[1] D. Hleis, M. Labaki, H. Laversin, D. Courcot, A. Aboukaïs, Colloids Surf. A 330 (2008) 193.
[2] V. Pârvulescu, P. Grange, B. Delmon, Catal. Today 46 (1998) 233.
[3] J. Ma, Y. Zhu, J. Wei, X. Cai, Y. Xie, Stud. Surf. Sci. Catal 130 (2000) 617.
[4] M. Labaki, S. Siffert, J. Lamonier, E.A. Zhilinskaya, A. Aboukaïs, Appl. Catal. B 43 (2003) 261.
[5] M. Haneda, Y. Kintaichi, M. Inaba, H. Hamada, Catal. Today 42 (1998) 127.
[6] T. Holma, A. Palmqvist, M. Skoglundh, E. Jobson, Appl. Catal. B 48 (2004) 95.
[7] M. Wojciechowska, M. Zielinski, W. Przystajko, M. Pietrowski, Catal. Today 119 (2007) 44.
[8] A. Fritz, V. Pitchon, Appl. Catal. B 13 (1997) 1.
[9] S. Wisniewski, J. Belkouch, L. Monceaux, C. R. Chimie 3 (2000) 443.
[10] A. Bueno-Lopez, J. Soriano-Mora, A. Garcia-Garcia, Catal. Commun 7 (2006) 678.
[11] H. Laversin, D. Courcot, E. Zhilinskaya, R. Cousin, A. Aboukaïs, J. Catal 241 (2006) 456.
[12] M. Labaki, J.F. Lamonier, S. Siffert, E.A. Zhilinskaya, A. Aboukaïs, Colloids Surf. A 227 (2003) 63.
[13] F. Wyrwalski, J.F. Lamonier, S. Siffert, L. Gengembre, A. Aboukaïs, Catal. Today 119 (2007) 332.
[14] F. Wyrwalski, J.F. Lamonier, S. Siffert, A. Aboukaïs, Appl. Catal. B 70 (2007) 393.
[15] I. Matsukuma, S. Kikuyama, R. Kikuchi, K. Sasaki, K. Eguchi, Appl. Catal. B 37 (2002) 107.
[16] J. Matta, J.F. Lamonier, E. Abi-aad, E. Zhilinskaya, A. Aboukaïs, Phys. Chem. Chem. Phys 1 (1999) 4975.
[17] G. Mul, F. Kapteijn, J.A. Moulijn, Carbon 37 (1999) 401.
[18] E. Saab, E. Abi-aad, M. Bokova, E. Zilinskaya, A. Aboukaïs, Carbon 45 (2007) 561.
[19] J.F. Lamonier, M. Labaki, F. Wyrwalski, S. Siffert, A. Aboukaïs, J. Anal. Appl. Pyrolysis 81 (2008) 20.
[20] K. Parida, H.K. Mishra, J. Mol. Catal. A Chem 139 (1999) 73.
[21] Z. Liu, W. Ji, L. Dong, Y. Chen, J. Solid State Chem 138 (1998) 41.
[22] S. Liu, S. Huang, L. Guan, J. Li, N. Zhao, W. Wei, Y. Sun, Microporous Mesoporous Mater. 102 (2007) 304.
[23] I.D. Lick, A.L. Carrascull, M.I. Ponzi, E.N. Ponzi, Ind. Eng. Chem. Res 47 (2008) 3834.
[24] P.W. Park, J.K. Kil, H.H. Kung, M.C. Kung, Catal. Today 42 (1998) 51.
[25] K. Ito, K. Kishikawa, A. Watajima, K. Ikeue, M. Machida, Catal. Commun 8 (2007) 2176.
[26] M. Labaki, J.F. Lamonier, S. Siffert, F. Wyrwalski, A. Aboukaïs, Thermochim. Acta 443 (2006) 141.
[27] C. Chien, T. Huang, Ind. Eng. Chem. Res 34 (1995) 1952.
[28] S. Aouad, E. Abi-Aad, A. Aboukaïs, Appl. Catal. B 88 (2009) 249.
[29] M. Jeguirim, V. Tschamber, J. Brilhac, P. Ehrburger, J. Anal. Appl. Pyrolysis 72 (2004) 171.